

Thermolysis of orthonovolacs. Part 1. Phenol–formaldehyde and *m*-cresol– formaldehyde resins¹

M.S. Chetan², R.S. Ghadage, C.R. Rajan, V.G. Gunjekar
and S. Ponrathnam*

*Polymer Science and Engineering Group, Chemical Engineering Division, National
Chemical Laboratory, Pune-411 008 (India)*

(Received 29 October 1992; accepted 10 December 1992)

Abstract

A sequence of phenol–formaldehyde and *m*-cresol–formaldehyde orthonovolac resins were synthesized by varying the mole ratios of phenol or substituted phenol to formaldehyde. The resins were characterized by their thermal properties such as softening temperatures and degradation profile. The non-isothermal procedures of Coats–Redfern and Horowitz–Metzger were applied to their respective differential thermogravimetric plots to ascertain the thermal degradation kinetics of these resins in air. The thermal stability and activation energies (E) of *m*-cresol–formaldehyde resins in the terminal degradation stage were correlated with those of the phenol–formaldehyde resins. The effect of aromatic ring substitution on the thermal stability is also discussed.

INTRODUCTION

Phenol–formaldehyde resins have been examined extensively, from commercial perspectives, over the past five decades because of their unique combination of properties. The phenol–formaldehyde (PF) orthonovolacs and their related derivatives form a major constituent of the positive photoresist formulations used in optical lithography [1–3]. Orthonovolacs, the weak-acid-catalysed oligomeric condensation products of phenols or substituted phenols and formaldehyde, have a linear structure and are permanently fusible. *m*-Cresol resins are selected for microelectronic applications because of their enhanced softening temperatures which lead to a decreased processing time and increase the throughput. Methyl substitution at the meta position amplifies the reactivity of phenol.

* Corresponding author.

¹ NCL communication No. 5264.

² Present address: Dept. of Plastics Eng., University of Lowell, Lowell, MA 01854, USA.

Moreover, cresol resins have a greater, desired moisture resistance than the phenolic resins.

In the present investigation, we report the synthesis of a number of phenol–formaldehyde (PF) and *m*-cresol–formaldehyde (CF) orthonovolac resins. The consequences of resin composition on softening temperature, the 10% and 25% degradation temperatures (10% DT and 25% DT), and the activation energy (E) of thermal degradation are discussed. The comparative performance of PF and CF resins is reported.

EXPERIMENTAL

Analytical reagent grade *meta*-cresol, phenol, formalin and oxalic acid were used as received. The formaldehyde concentration in formalin was estimated by a standard procedure. The phenol to formaldehyde mole ratio was varied in different reactions between 1.00:0.80 and 1.00:1.05. Oxalic acid was used as the catalyst. In the second set of experiments, *m*-cresol was reacted with formaldehyde. The *m*-cresol to formaldehyde mole ratio was varied between 1.00:0.60 and 1.00:1.05.

The polycondensations were conducted in a 500 cm³ 4-necked round-bottomed flask at 90°C for 6 h with constant stirring. The unreacted monomers were distilled out at reduced pressure at elevated temperature to obtain the resin. The resins were dried in a desiccator over phosphorous pentoxide. The softening temperatures were estimated in sealed glass capillaries on a melting point apparatus.

The thermal behaviour of the resins was studied in air using a Netzch STA-409 thermogravimetric analyser. The approximate sample size was 20 mg. Resins were heated at the constant rate of 10°C min⁻¹. Thermograms were obtained in the range 25–900°C.

RESULTS AND DISCUSSION

The softening point of a resin is of critical importance in photolithographic processing. Coated resists are baked prior to and after exposure to radiation. This baking temperature is kept below the softening point so as to ensure that the resin does not flow after image transfer. However, a higher softening point is necessary to enhance the baking temperatures, to decrease the baking cycle time and to increase the throughput. The softening temperatures of PF (4 compositions) and CF orthonovolac resins (5 compositions) are shown in Table 1. The incorporation of a methyl group in the aromatic ring increases the softening temperature, on average by 25°C.

The shape of a TGA thermogram primarily depends on the reaction order (n), the pre-exponential factor (A) and the energy of activation (E)

TABLE 1

Thermal properties of orthonovolac resins

No.	Sample code	HCHO mole ratio	Temperature/°C					
			Softening	T_i	T_f	ΔT	10% DT	25% DT
1	PF 105	1.05	96–99	367.4	649.0	281.6	405.2	512.4
2	PF 100	1.00	87–90	324.1	664.4	240.3	391.8	483.7
3	PF 090	0.90	74–78	328.5	634.5	306.0	385.8	474.2
4	PF 080	0.80	62–66	246.5	645.1	398.6	316.5	413.8
5	MF 105	1.05	123–126	181.4	716.2	534.8	359.5	394.9
6	MF 100	1.00	115–117	180.0	686.6	506.6	369.8	413.5
7	MF 090	0.90	100–104	161.2	808.0	646.8	361.4	413.0
8	MF 080	0.80	87–90	117.0	748.0	631.0	312.2	377.4
9	MF 060	0.60	69–72	149.3	803.7	654.5	311.8	362.5

Key: T_i , initial degradation temperature; T_f , final degradation temperature; $\Delta T = T_f - T_i$, temperature range over which degradation is observed; DT, degradation temperature, PF, phenol–formaldehyde series, MF, *m*-cresol–formaldehyde series.

[4]. The TGA thermograms of multistage degradations are more intricate. The slope of a TGA trace at a particular temperature relates to the rate of degradation. It is fairly difficult to judge slopes in the steep regions of TGA traces. Such situations are nullified by the application of differential thermogravimetry (DTG). Here, the degradation rate is depicted by the height of a DTG curve above the base line. The DTG curve ensures the feasibility of estimating the temperature of the maximum degradation rate (T_{max}), the initial degradation temperature (T_i) and the final degradation temperature (T_f) [5]. The area under a DTG peak is directly proportional to the extent of mass change during degradation. Hence, DTG thermograms are used for thermal stability analysis. The thermal degradations in air of four PF resins and five CF resins were examined in the 100–800°C range. The superimposed plots of the rate of change in mass of the PF and CF resins are presented in Figs. 1 and 2, respectively.

PF resins are stable up to 230–330°C. This thermal stability is dependent on the composition of the resin. Replacing phenol with *m*-cresol yields a significant decrease in the thermal stability. The initial and final (T_i and T_f) degradation temperatures for these two resin series are shown in Table 1. Incorporating a methyl substituent diminished the initial degradation temperature (T_i), on average by 150°C. The final degradation temperatures (T_f) in CF resins are higher than those of PF resins of similar compositions. Thus, the temperature range (ΔT) over which degradation is observed is wider for CF resins. The data based on qualitative methods, such as temperatures at 10% and 25% degradation (10% DT and 25% DT), are also presented in Table 1 and are depicted graphically in Fig. 3. Two

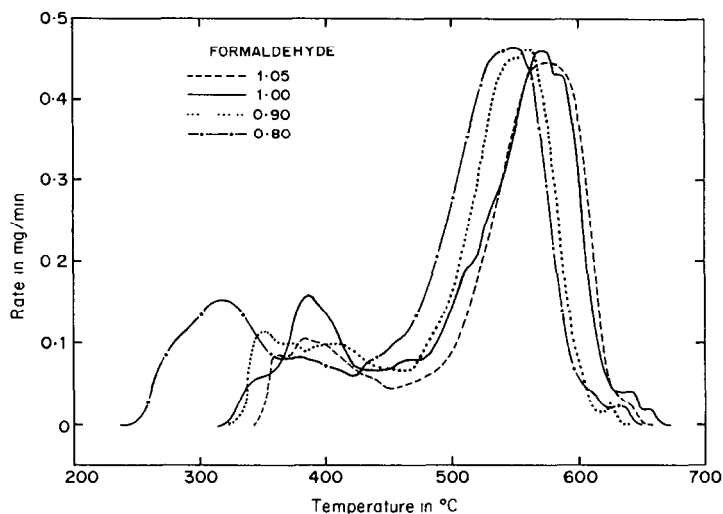


Fig. 1. DTG thermograms for the degradation of phenol-formaldehyde resins of various compositions.

salient features are apparent from the data: the thermal stability of CF resin is lower than that of PF resin by around 30°C; and the rate of thermal degradation is faster for CF resins. Also, in both series these temperatures fall with a decrease in the mole fraction of formaldehyde in the resin. The thermal stability dependence of PF resin on the concentration of the dihydroxy diphenyl methane moiety has been documented [6]. The

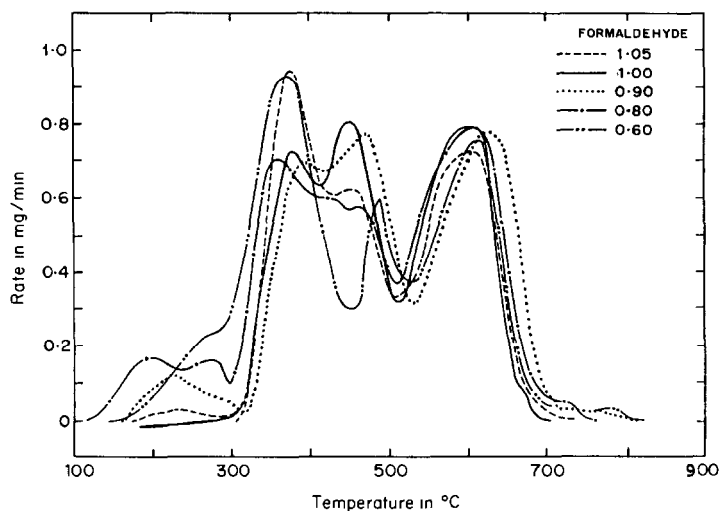


Fig. 2. DTG thermograms for the degradation of *m*-cresol-formaldehyde resins of various compositions.

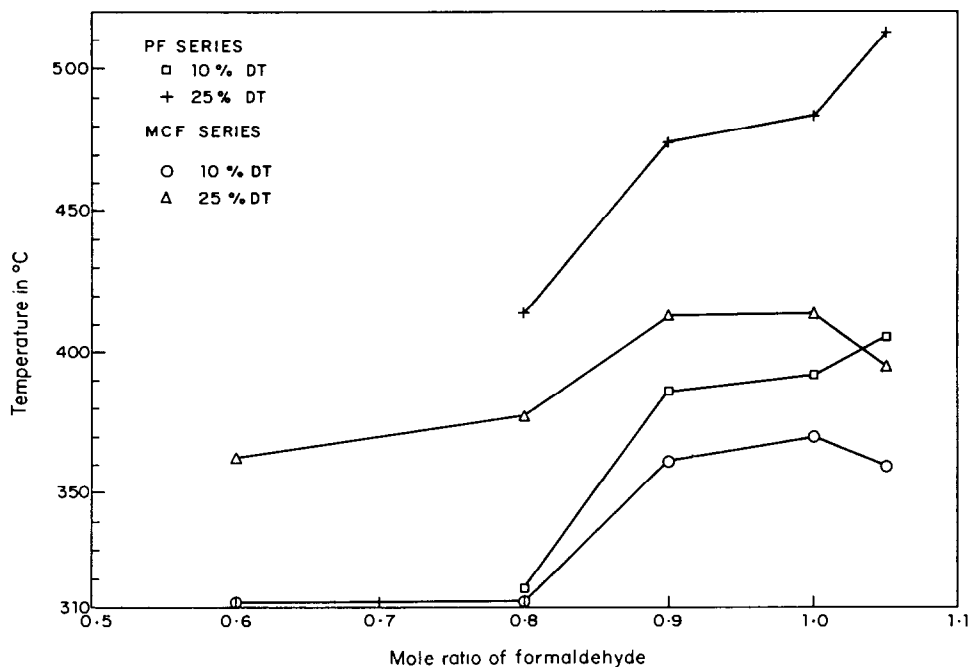


Fig. 3. Plot of the mole ratio of formaldehyde against decomposition temperatures (10% DT and 25% DT).

methylene linkages are generated by the condensation of formaldehyde. The number of such linkages are dictated by its mole fraction in the resin.

The degradation of PF resins occurs in two distinct stages (Fig. 1). Three degradation stages, namely initial, intermediate and final, are observed in CF resins (Fig. 2). In each thermogram, there is a sharp break after an initial weight loss, which indicates the onset of a decomposition profile, with the rapid loss of volatile fragments.

The degradation of the PF resins starts at around 250°C, becoming relatively rapid above 500°C. The weight loss is 20–30% in the initial stage (250–450°C), arising from the volatilization of bound water and other low molecular weight species [7]. The final degradation stage, observable beyond 500°C, becomes relatively rapid at 550°C and is complete at 650°C.

The degradation of CF resins occurs in three stages. The initial and intermediate stages are observed in the 100–450°C and 450–550°C temperature ranges respectively. The final degradation stage occurs beyond 550°C, and is complete around 800°C. The final stage is the most prominent in both series and is observable over similar temperature ranges, irrespective of composition and chemical structure [8]. This final stage was selected for comparison in terms of the effects of composition and structure on the energy of activation E .

It is essential to estimate the area under a DTG peak to evaluate the

kinetic parameters of degradation. The area estimation should be intrinsically correct, especially when peaks emanating from interfering reactions overlap significantly. The method of Anderson and Freeman was used in this analysis [9].

The activation energies of degradation E were estimated from the DTG curves using the following non-isothermal integral equations to evaluate the kinetic parameters:

(a) the Coats–Redfern equation I (CR I) [10]

$$\log\left(\frac{1 - (1 - \alpha)^{1-n}}{(1-n)T^2}\right) = \log\frac{AR}{aE}\left(1 - \frac{2RT}{E}\right) - \frac{E}{2.303 RT} \quad (1)$$

(b) Coats–Redfern equation II (CR II)

$$\log\left(\frac{-\ln(1 - \alpha)}{T^2}\right) = \log\frac{AR}{aE}\left(1 - \frac{2RT}{E}\right) - \frac{E}{2.303 RT} \quad (2)$$

(c) Horowitz–Metzger method (HM) [11]

$$\ln(-\ln(1 - \alpha)) = E\theta/RT_s^2 \quad (3)$$

where $\alpha = (W - W_f)/(W_o - W_f)$ (W_o , W_f and W are the initial mass, final mass and mass remaining at temperature T (equivalent to the final degradation stage)), $\theta = T - T_s$, and T_s is the temperature at $W/W_o = 1/e$.

The equation CR II is valid for reactions with an order parameter n of unity, and CR I is applicable for reaction order parameters other than unity.

The order parameter n was evaluated using CR I and CR II. The plots of the left-hand-side function (LHS) versus $1/T$ were drawn for different values of n in the range 0–3, excepting for $n = 1$; CR II was used for $n = 1$. The superimposed plots of the LHS function of CR I or CR II versus $1/T$ are presented in Fig. 4. For $n = 1$ and 3 (CR I), a linear relationship was not observed, whereas for $n = 1$ (CR II), $\log[-\ln(1 - \alpha)]$ against $1/T$ was linear. This indicates that degradation in the last stage followed first-order kinetics. This was confirmed by the Horowitz–Metzger (HM) equation.

The plot of $\log[\ln(1 - \alpha)^{-1}/T^2]$ versus $1/T$ (CR II) and $\ln[-\ln(1 - \alpha)]$ versus θ (HM equation) were plotted and the energy of activation E was evaluated from the slope of the straight lines for the nine resin samples. The correlation coefficients r for the plots were also determined in each case. These were found to be near unity for the eighteen plots, reflecting the linearity of the curves.

Superimposed plots for the final degradation stage of PF and CF resins of $\log[\ln(1 - \alpha)^{-1}/T^2]$ against $1/T$ (CR plots) are represented in Figs. 5 and 6, respectively. The temperature ranges and extent of degradation within which the analyses were conducted are shown in Table 2. Here, the presented extent of degradation pertains only to that in the last

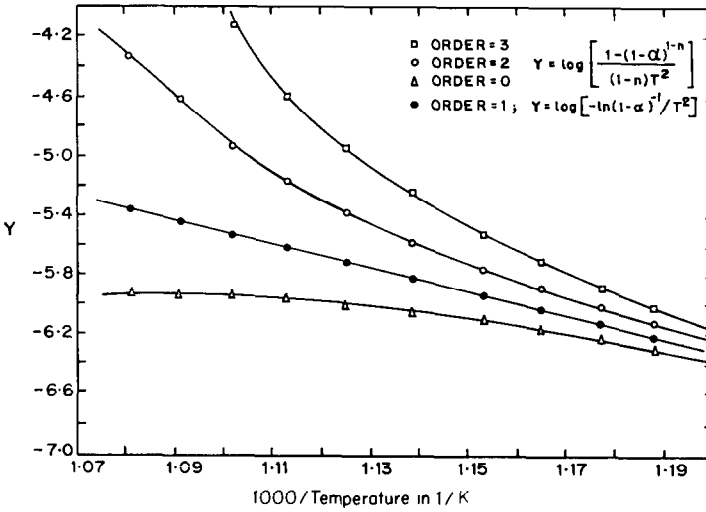


Fig. 4. Coats–Redfern plots for *m*-cresol–formaldehyde (1:1) resin at $n = 0, 1, 2$ and 3 .

degradation stage. The kinetic parameters for the nine resins were analysed in the 25–95% degradation range. The initial 25% degradation zone was not considered in order to avoid errors due to overlap from the previous degradation zone [12]. It is also known that in the initial stages, the decomposition of solids do not obey first-order kinetics.

Similarly, the superimposed plots of the final degradation stage for PF and CF resins of $\ln[-\ln(1 - \alpha)]$ against θ (HM plots) are shown in Figs. 7

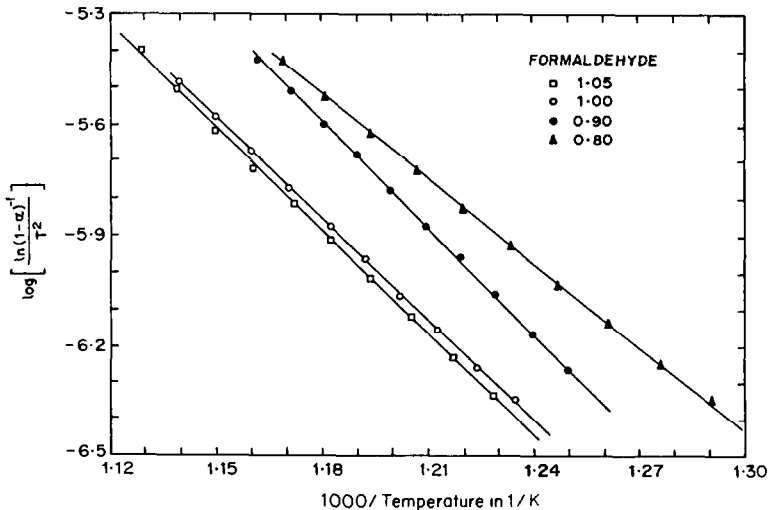


Fig. 5. Coats–Redfern plots for phenol–formaldehyde resins of various compositions (last stage of degradation).

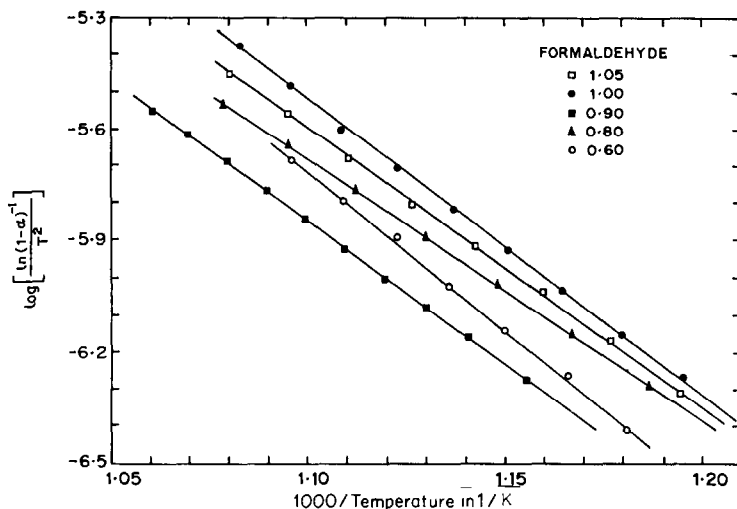


Fig. 6. Coats-Redfern plots for *m*-cresol-Formaldehyde resin of various compositions (last stage of degradation).

and 8, respectively. The activation energies E calculated for these resins are given in Table 2. The activation energy E was computed from the slopes of the Coats-Redfern and Horowitz-Metzger plots. There is no apparent relationship between activation energies E and formaldehyde content in these two orthonovolac series. This is probably due to variations in the molecular weights of the resins [13].

TABLE 2

Decomposition activation energies in the final stage for orthonovolac resins

No.	Sample code	HCHO mole ratio	Analysis range				Energy of activation/ (kJ mol ⁻¹)	
			Temperature/°C		Decomposition/%		HM	CR
			Start	End	Start	End		
1	PF 105	1.05	536.5	616.9	23.3	97.1	190.8	176.0
2	PF 100	1.00	532.8	611.7	22.5	94.8	188.2	172.4
3	PF 090	0.90	523.9	587.6	25.2	93.9	199.6	185.4
4	PF 080	0.80	497.5	582.5	20.4	93.4	162.6	146.1
5	MF 105	1.05	559.4	652.8	25.5	95.1	157.5	142.9
6	MF 100	1.00	560.6	657.8	28.1	98.4	164.8	152.7
7	MF 090	0.90	592.3	675.2	32.4	93.5	159.3	145.7
8	MF 080	0.80	560.4	654.2	24.0	91.7	150.8	134.6
9	MF 060	0.60	574.0	645.1	23.9	86.0	180.4	162.6

Key: HM, values obtained by Horowitz-Metzger method; CR, values obtained by Coats-Redfern method; PF, phenol-formaldehyde series; MF, *m*-cresol-formaldehyde series.

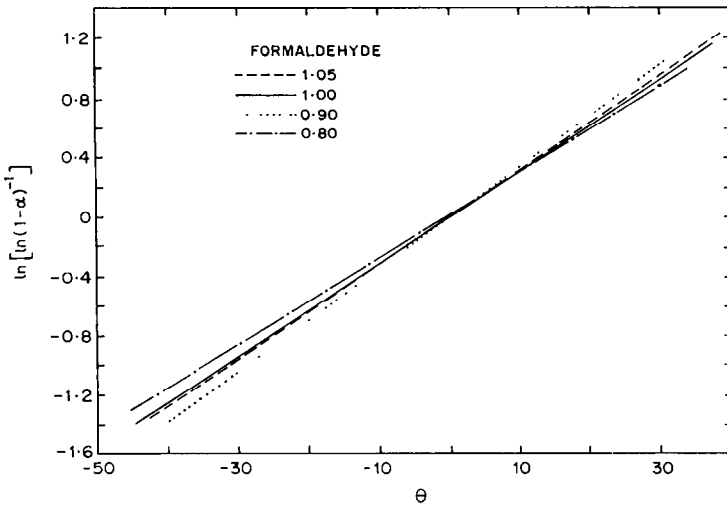


Fig. 7. Horowitz–Metzger plots for phenol–formaldehyde of various compositions (last stage of degradation).

The first-order reactions have an overall activation energy E in the range of 150–200 kJ mol⁻¹ for PF resins and 130–180 kJ mol⁻¹ for CF resins. The decrease in activation energy E of the PF resin with formaldehyde content is comparable with literature values [14, 15]: activation energy is known to decrease with a reduction in the molecular weight of the sample [16]. The lower energy of activation E of the PF resins studied here, compared to literature data, reflects the lower molecular weight of the resins examined in the present study.

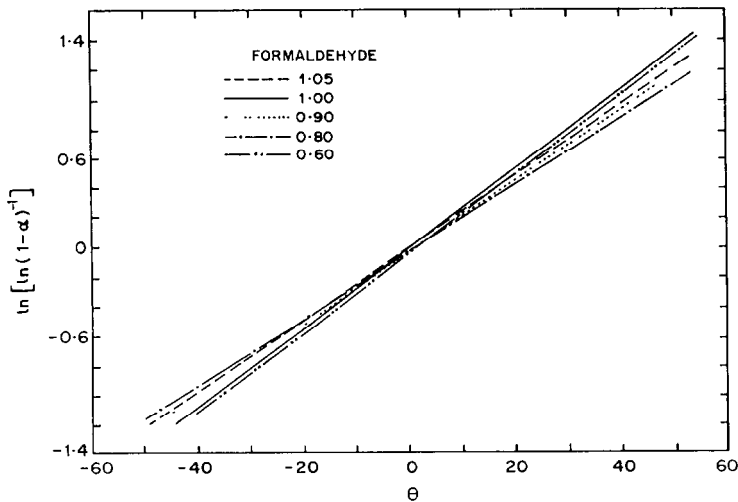


Fig. 8. Horowitz–Metzger plots for *m*-cresol–formaldehyde resins of various compositions (last stage of degradation).

The activation energies calculated by the Coats–Redfern and Horowitz–Metzger methods are listed in Table 2. The higher activation energies E estimated by the HM method result from the approximation in its derivation [17]. At identical compositions, the activation energies E of CF resins are lower than those from the PF series. The thermal degradation at higher temperature is primarily related to the stability of the dihydroxy diphenyl methane moieties in phenol/substituted phenol–formaldehyde resins [6]. Methyl substitution at the meta position of phenol in *m*-cresol results in a change in the stability of the dihydroxy diphenyl methane unit. Hence, the lower thermal stability of *m*-cresol–formaldehyde resins is probably due to the lower inherent stability of the 2,2'-dihydroxy-6,6'-dimethyl diphenyl methane unit.

ACKNOWLEDGEMENT

This project was funded by the Department of Electronics, New Delhi 110 003, India.

REFERENCES

- 1 F.A. Volenbrock and E.J. Spiert, *Adv. Polym. Sci.*, 94 (1988) 85.
- 2 S.R. Turner and R.C. Daly, *J. Chem. Educ.*, 65 (1988) 332.
- 3 A. Kumar, U.K. Phukan, A.K. Kulshrestha and S.K. Gupta, *Polymer*, 23 (1982) 215.
- 4 L. Reich and D.W. Levi, in A. Peterine, M. Goodman, S. Okamura, B.H. Zimm and H.F. Mark, (Eds.), *Macromolecular Reviews*, Vol. 1, Interscience, New York, 1965, p. 174.
- 5 A.W. Coats and J.P. Redfern, *Analyst*, 88 (1963) 906.
- 6 R.T. Conley, H.W. Lochte and E.L. Strauss, *J. Appl. Polym. Sci.*, 9 (1965) 2799.
- 7 M. Tugtepe and S. Ozgumus, *J. Appl. Polym. Sci.*, 39 (1990) 83.
- 8 K.D. Jeffreys, *Br. Plast.*, 36 (1963) 188.
- 9 D.A. Anderson and E.S. Freeman, *J. Appl. Polym. Sci.*, 1 (1959) 192.
- 10 A.W. Coats and J.P. Redfern, *Nature*, 201 (1964) 68.
- 11 H.H. Howoritz and G. Metzger, *Anal. Chem.*, 35 (1963) 1464.
- 12 A.W. Coats and J.P. Redfern, *J. Polym. Sci. Part B*, 3 (1965) 917.
- 13 M.S. Chetan, B. Eng. Dissertation, University of Poona, Pune, India, 1987.
- 14 G.P. Shulman and H.W. Lochte, *J. Appl. Polym. Sci.*, 10 (1966) 619.
- 15 H.L. Friedman, *J. Polym. Sci. Polym. Symp.*, 6 (1964) 183.
- 16 B.V. Kokta, J.L. Volade and W.N. Martin, *J. Appl. Polym. Sci.*, 17 (1973) 1.
- 17 C.G.R. Nair and K.N. Ninan, *Thermochim. Acta*, 23 (1978) 161.